

# ENHANCED EXPONENTIAL REACHING LAW-BASED SLIDING MODE CONTROL OF SHUNT ACTIVE POWER FILTER IN AN ELECTRICAL DISTRIBUTION SYSTEM

Vinay Kumar Naguboina<sup>1</sup> and Satish Kumar Gudey<sup>2,\*</sup>

<sup>1</sup> Vignan's Institute of Information Technology, Andhra Pradesh, India,

<sup>2</sup> Gayatri VidyaParishad College of Engineering (Autonomous), Andhra Pradesh, India

**ABSTRACT:** In this work, a three-phase Shunt Active Power Filter (ShAPF) is proposed to address the current related issues in a three-phase Electrical Distribution System (EDS). A sliding mode controller (SMC) and an Enhanced Exponential Reaching Law-based SMC (EERL-SMC) are proposed for a ShAPF to compensate for the load current. The controller's performance is tested by injecting the current harmonics into the system. A non-linear load along with different loads on the distribution side is connected in parallel in a distribution network at the point of common coupling (PCC). Modelling of the system is done using state-space analysis. The stability of the system is analyzed using the state feedback approach. The reference source currents are generated using the instantaneous  $PQ$  theory. For variations in the load, the THD in the source current is realized. It is found that EERL-SMC is more effective for a ShAPF in reducing the high-frequency oscillations and settling time for convergence. The source voltage and current waveforms are observed to be sinusoidal. Both the controllers are effective in reducing the THD levels in the source current as per the IEEE standards. A comparison between the controllers is presented in terms of settling time, THD in source current. PSCAD v4.6 is used for simulation works.

**Keywords:** Electrical Distribution System (EDS); Shunt Active Power Filter (ShAPF); Point of Common Coupling (PCC); Total Harmonic Distortion (THD); Sliding Mode Controller (SMC); Enhancement Exponential Reaching law (EER-Law).

## وحدة التحكم بالإنزلاق المبنية على قانون الوصول الآسي المحسن لمرشح القدرة الفعالة المتوازي في شبكة التوزيع الكهربائي

فيماي كومار ناغوبينا<sup>1</sup> و ساتيش كومار جودي<sup>2,\*</sup>

**المخلص:** يقدم هذه البحث مقترحا لاستخدام مرشح للقدرة الفعالة ذو ثلاثة أوجه تصفية لحل مشاكل شبكات توزيع الكهرباء ذات الثلاثة أوجه، كما يقترح استعمال وحدة التحكم بوضع الانزلاق بنسختها العادية والمبنية على قانون الوصول الآسي المحسن لتعويض تيار الحمل في مرشح للقدرة الفعالة المتوازي ذو ثلاثة أوجه، حيث يتم اختبار اداء وحدة التحكم بحقق النظام بتوافقيات التيار. تم توصيل حمل خطي وأحمال اخرى مختلفة بالتوازي في شبكة توزيع الكهرباء عند نقاط الربط المشتركة، ووضع نموذج النظام عن طريق التمثيل المصفوفي للمعادلات التفاضلية، كما تم تحليل استقرار النظام عن طريق نهج التغذية الراجعة للحالة، ويتم انشاء تيارات المصدر المرجعي باستخدام النظرية المعممة للقوة التفاعلية اللحظية في الدوائر ثلاثية الطور، كما تحقق تشوه توافقي كلي في التيار المصدر نتيجة لاختلاف الحمل. اشارت نتيجة الدراسة الى ان وحدة التحكم بالانزلاق المبنية على قانون الوصول الآسي المحسن تعطي تأثيرا اكبر في تقليل ذبذبات التردد العالي وزمن السكون في مرشح القدرة الفعالة ذو ثلاثة أوجه، كما لوحظ أن جهد المصدر وأشكال موجة التيار هي جيبيية بطبيعتها. نجح كلا من وحدتي التحكم بالانزلاق في تقليل التشوه التوافقي الكلي في مصدر التيار كما ورد في معايير معهد مهندسي الكهرباء والإلكترونيات. كما تم في هذه الورقة عرض مقارنة بين نوعي وحدات التحكم بالانزلاق وُضح من خلالها زمن السكون والتشوه التوافقي الكلي في مصدر التيار.

**الكلمات المفتاحية:** شبكة توزيع الكهرباء؛ مرشح التوازي للقدرة الفعالة ذو ثلاثة أوجه؛ نقاط الربط المشتركة؛ وحدة التحكم بالإنزلاق؛ تشوه توافقي.

\*Corresponding author's e-mail: satishgudey5@gvpce.ac.in



## 1. INTRODUCTION

The Electrical Distribution System (EDS) consists of different types of loads like linear loads, non-linear loads and sensitive loads. At the point of common coupling, all these loads are connected in parallel. Among these loads, non-linear loads inject current harmonics into the electrical distribution system (EDS). This increases the Total Harmonic Distortion (THD) percentage in current at the PCC. This will cause a huge amount of impact on the performance of both sensitive loads and linear loads and may also damage these loads. The usage of non-linear loads like computers, Televisions, Printers etc. has been increasing day by day and hence, increases non-linearity in source current. These non-linear currents will adversely affect the system voltage. If such voltages are supplied to the loads then the system performance will be drastically affected (Thentral, T. M. T. *et al.*, 2021).

The problem of non-linearity is mainly because of the non-linear loads connected at PCC. These loads have to be isolated from the linear and sensitive loads to prevent the voltage and current distortions, which is not practically possible. Hence, proper preventive measures have to be taken to protect these linear and sensitive loads from the source voltage and current distortions. This has led the researchers to design compensating devices that will protect these loads. Passive filters are conventional filters that can be designed to protect the loads from the harmonics.

The development of power semiconductor devices and signal processing devices and availability at reduced cost have attracted researchers to work with active filters (AF). AF can perform numerous functions like harmonic filtering, damping, voltage regulation, load balancing and other power quality issues arising in a distribution system. AF's are further categorized as pure active power filters (PAF) and Hybrid active power filters (HAF). PAF's mainly consists of only one single voltage source converter fed with a DC capacitor. HAF includes multiple or single voltage source PWM converters with passive filters like inductor and capacitor and/or resistors. Generally, for high power applications, HAF is more commonly used for harmonic mitigation in terms of performance and cost.

In this work, a shunt active power filter for harmonic mitigation is presented in a distribution system with the mathematical model and stability analysis. The main contributions of this work are as follows (i) A ShAPF has been designed and simulated to protect the sensitive loads from current distortions. (ii) Enhancement Exponential Reaching law (EER-Law) is added to the conventional SMC controller to improve the performance of the system. (iii) A comparative analysis is performed in THD's of the source current with different loads. Section II discusses the Passive filters used for harmonic

mitigation.

## 2. PASSIVE AND ACTIVE POWER FILTERS

There are different kinds of passive filters like low pass filters, high pass filters, single tuned filters, double-tuned filters etc. These filters consist of passive elements like resistors, inductors and capacitors (S. M. Mozayan *et al.* 2016). As shown in Fig. 1,  $R, L, C$  values should be calculated based upon the formulas given in (1).

$$\left. \begin{aligned} C &= Q_c / (6.28 V f^2) \\ X &= 1 / (6.28 f h C) \\ L &= X / 2 h f \\ Q &= 6.28 f L / R \\ R &= 1 / 6.28 f C \end{aligned} \right\} \quad (1)$$

where  $Q_c$ = reactive power of filter (MVAR),  $V$ = supply voltage (V),  $Q$  = quality factor,  $h$  = tuning harmonic order of the filter,  $f$  is the power frequency.

The tuned low pass filter and high pass filters will eliminate the harmonics based upon their cut-off frequency. The designed single tuned filter will eliminate the particular harmonic for which it is tuned. The dominant frequency harmonic component has to be identified in supply voltage or current. This can be done by using Fast Fourier Transforms (FFT) Analysis. The filter has to be designed in such a way as to eliminate that harmonic component in voltage or current. The designed filter has to be connected in parallel to the load so that it acts as a conductance path for that harmonic component. Similarly, it should also act as a high impedance path for the remaining harmonic components. Thus, the harmonic components are deviated through passive filters without reaching the loads. Thus, the percentage of THD in load voltage and current will be decreased. Thus, by using the single tuned filters the THD can be reduced.

Similarly, if the two frequency components are found to be dominant then double-tuned filters are preferred. These filters are designed to eliminate the two harmonic frequency components. The main drawback of passive filters is the presence of resonance between the line and the filters. If the impedance of the designed filter and system impedance is equal then the system is said to be in resonance condition. This will inject the abnormal disturbances line noise into the system. The basic drawback of these passive filters is that they can eliminate only the single or double frequency components. For any variations in the non-linear loads

that are in one condition, the harmonics occurring in the system will change dynamically. This made the researchers shift their focus towards the devices, which can provide dynamic and effective solutions (AlirezaJavadi *et al.* 2017).

Among the available different Active Power Filter (APF), Shunt Active Power Filter (ShAPF) and Series Active power filters (SeAPF) will function dynamically. These filters can provide effective solutions. The shunt Active power filter can mitigate the current harmonics and the series active power filter acts as a voltage regulator.

Unlike the traditional passive filters, APF will have the flexibility to provide multiple functions like eliminating multiple harmonic frequency components, injection of reactive power, correction of power factor, regulation of voltage and voltage flicker reduction etc.

Also due to the decrement in the manufacturing cost of power semiconductor devices and signal processing devices manufacturers have shown more interest in APF's (Alireza Javadi *et al.* 2016). However, the manufacturing cost of APF's is quite high when compared with the conventional passive filters. APF's are mainly classified into two types based upon their application. They are single-phase APF and 3- $\Phi$  APF. However, the usage of single-phase APF is only restricted to low-power applications. This made the researchers search for the device, which can be used in high power applications i.e. three-phase APF. In this paper, the performance of the three-phase shunt APF is analyzed through simulation works.

### 3. SHUNT ACTIVE POWER FILTER

These type of filters consists of Active Power Filter (APF) connected in shunt across the load. In this Active Power Filter, the voltage source current-controlled converter is used to inject the compensating current to suppress the distortions present in load voltage and load current (Sharma, S. *et al.* 2020). The distortions in load voltage and current are calculated separately and then the resultant total error is calculated by summing the voltage error and current error. The compensation is done by injecting the compensating current, which will suppress the distortions in voltage and current.

Figure 2 shows the schematic representation of the ShAPF. It consists of an AC power supply feeding a non-linear load. A shunt APF consisting of a voltage source inverter (VSI) connected in shunt at PCC to inject a shunt current to provide compensation against current harmonics.  $L_s$  and  $L_L$  are the source side and load side inductances, which play a key role in the compensation. Along with the sensitive loads, non-linear loads are always present in the distribution network  $L_{se}$  is the series winding inductance to the VSI and  $V_{dc}$  is the input DC voltage supply.

In the circuit shown in Figure 3, a three-phase Shunt Active Power Filter (ShAPF) is presented with a sliding mode controller (SMC), which consists of a

current-controlled VSC. This converter should insert the compensating current if needed. The compensating current will be with a phase shift of exactly 180 degrees to the distortion that occurred in the source current. Now to inject this compensating current the current-controlled voltage source converter should function dynamically and should be turned on instantly (Javadi, A. *et al.* 2017), (Javadi, A. *et al.* 2016). For this purpose, a controller should be designed in such a way that it should generate the firing pulses during the need for compensation.

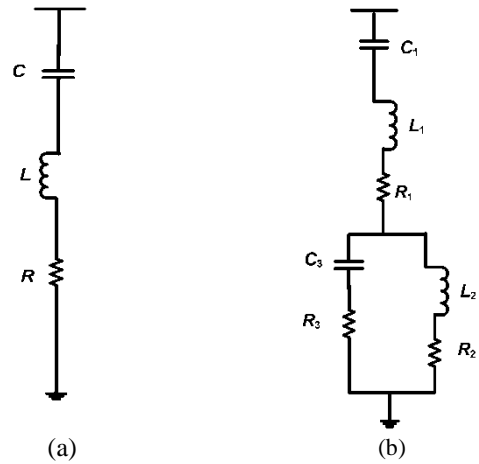


Figure 1. (a) Single tuned passive filter, and (b) Double tuned passive filter.

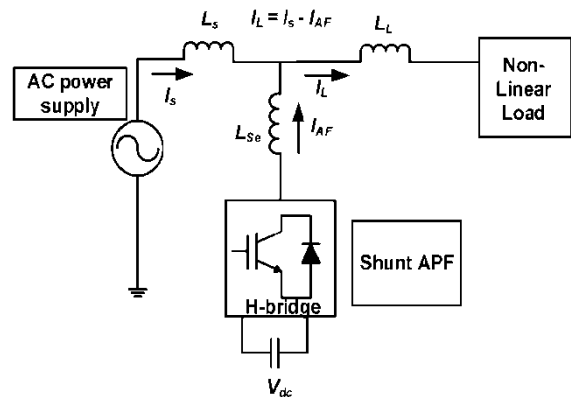


Figure 2. Schematic representation of ShAPF.

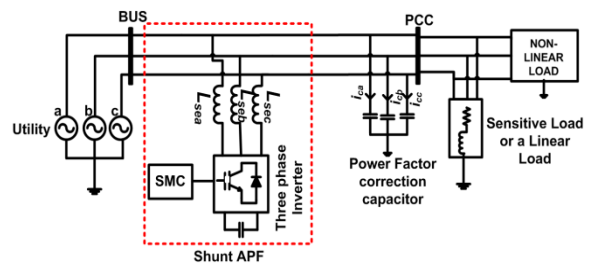


Figure 3. Block diagram of three-phase Shunt Active Power Filter.

#### 4. SMC WITH PQ THEORY

Figure 4(a) shows the SMC controller with a linear sliding surface. SMC is one of the robust non-linear controllers. It was used in many practical applications because of its simple construction and its accuracy. This SMC can vary the reference signals and can easily track the control signals dynamically when compared with other controllers. This SMC design mainly consists of two parts. One is choosing the sliding surface and the other is fine-tuning the sliding coefficients. In this proposed work, an SMC with a linear sliding surface is chosen and the sliding coefficient  $K_1$  value is chosen as 100. The equation for a linear sliding surface is presented in (4). This SMC is used to generate the firing pulses to the converter, which will inject the required compensating current. This compensating current is exactly a  $180^\circ$  phase shift to harmonics in the source current.

The instantaneous  $PQ$  theory is used to calculate the error in the source current. The actual and the reference values of the three-phase voltages and currents are converted into stationary reference frames. Then these voltages and currents are multiplied together to generate the actual and reference values of Active and Reactive power. Now the resultant error in powers is calculated by analyzing the real values with the reference values. The obtained  $P_{error}$  and  $Q_{error}$  are converted into their

respective phase current errors by using the Inverse Instantaneous  $PQ$  theory, (Ma, H. *et al.*, 2017). Thus, these obtained error signals are given to the pulse width modulator to generate the firing pulses at the desired instant. The switching frequency chosen is 10 kHz. Fig. 4 (b) shows the controller block diagram.

$$P = V_\alpha I_\alpha + V_\beta I_\beta \quad (2)$$

$$Q = V_\beta I_\alpha - V_\alpha I_\beta \quad (3)$$

$$\sigma_s = k_1(I_{ref} - I_{actual}) \quad (4)$$

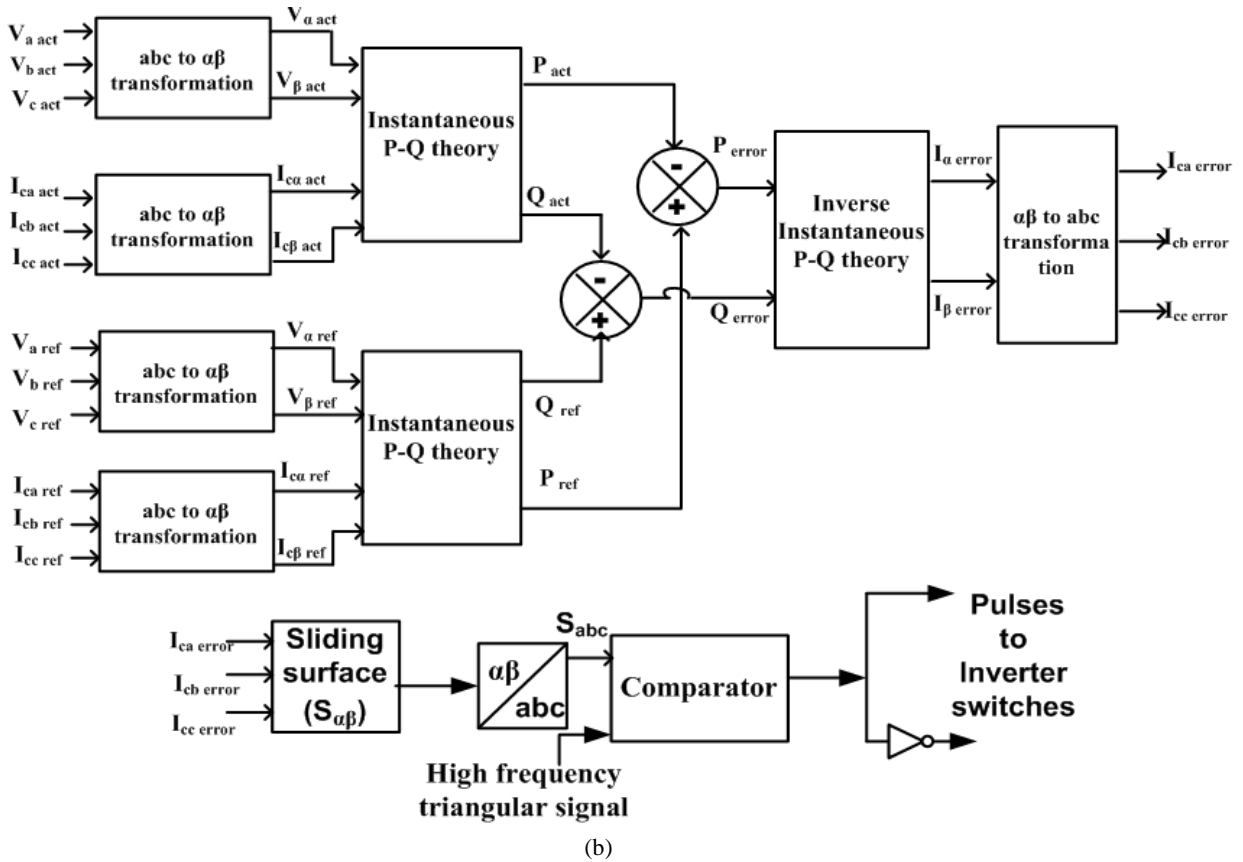
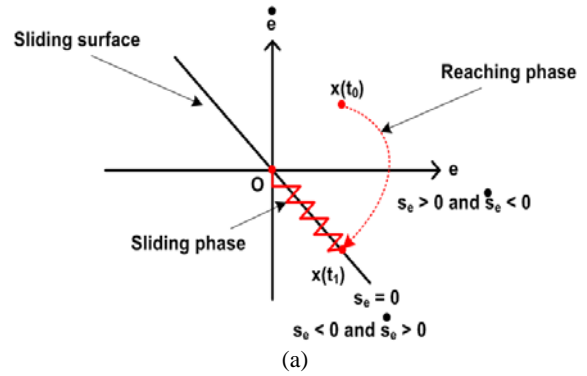


**Figure 4.** (a) Linear Sliding Surface  $\sigma_s$ , and (b) Schematic diagram of the controller for ShAPF.

## 5. MODELING OF SHUNT ACTIVE POWER FILTER USING STATE-SPACE ANALYSIS

To determine the stability of ShAPF, the state-space model is derived using state-space analysis. Figure 5 shows the equivalent circuit of ShAPF. The voltage across the load ( $V_L$ ), current injected by the ShAPF ( $i_{se}$ ) and current through the power factor correction capacitor ( $i_c$ ) have been considered as state variables. The controller can be designed by considering any one of the state variables as a controlling parameter. In this proposed controller the current through the power factor correction capacitor is considered as the controlling parameter (M. H. Rashid, 2011). The frequency response characteristics of the designed system are obtained and its stability margins are analyzed.

$$\dot{x} = Ax + b_1u + b_2V_s + b_3i_L \quad (5)$$

$$y = Cx \quad (6)$$

The state feedback approach is used to obtain the frequency response characteristics. The state model is represented in (7). The transfer function obtained for the system considered in the open-loop condition is represented in (8).

$$\begin{bmatrix} \dot{v}_L \\ \dot{i}_c \\ \dot{i}_{se} \end{bmatrix} = \begin{bmatrix} 0 & \frac{1}{C} & 0 \\ 0 & -\frac{1}{L_s} - \frac{1}{L_L} & -\frac{R_s}{L_s} \\ 1 & 0 & -\frac{R_{se}}{L_{se}} \end{bmatrix} \begin{bmatrix} v_L \\ i_c \\ i_{se} \end{bmatrix} + \begin{bmatrix} 0 \\ 0 \\ \frac{V_{dc}}{L_{se}} \end{bmatrix} u + \begin{bmatrix} 0 \\ \frac{1}{L_s} V_s + \left[ -\frac{R_s}{L_s} + \frac{R_L}{L_L} \right] i_L \\ 0 \end{bmatrix} \quad (7)$$

$$G(s) = C(sI - A)^{-1}b_1 \quad (8)$$

where  $A$  is the state matrix of order  $3 \times 3$ ,  $b_1$  is the input matrix of order  $3 \times 1$ ,  $b_2$  is the source voltage matrix of order  $3 \times 1$ ,  $b_3$  is the load current matrix of order  $3 \times 1$ ,  $C$  is the output matrix i.e.  $C = [0 \ 1 \ 0]$ . From the gain margin and phase margins acquired from the bode plots, it can be concluded that the system is stable. The transfer function obtained is given in (9).

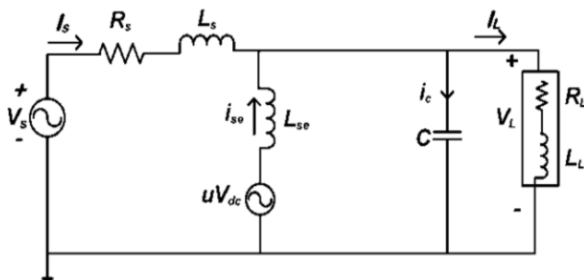


Figure 5. Equivalent circuit for shunt APF.

$$G(s) = \frac{-1e08s}{s^3 + 5.002e05s^2 + 3.535e-09s + 2.193e06} \quad (9)$$

It is found that a GM of infinity and a PM of 90 degrees is obtained for the designed system, which can be considered as a stable system with high stability margins. The controller works effectively with the chosen state variable.

Table 1 represents the configuration parameters. The rating of the ShAPF is 1.431 kVA for a three-phase distribution system.

## 6. SIMULATION RESULTS

The work considers different types of loads (like linear, non-linear and sensitive loads) in the electrical distribution network for simulation analysis. The current drawn from the source is shown in Fig. 7. The non-linear load representation is shown in Fig. 8(a). All three phases of the source current are said to be non-linear. The nonlinear load considered is a three-phase thyristor bridge rectifier with different combinations of loads on the DC side (Ouchen, S *et al.* 2021), (Satish Kumar Gudey *et al.* 2014). The magnitude of the load current is 10 A (peak/phase).

Table 1. System Parameters.

| Symbol             | Definition                         | Value                 |
|--------------------|------------------------------------|-----------------------|
| $V_s$              | Supply voltage (L-N)               | 141.4 (max)           |
| $f$                | Supply frequency                   | 50 Hz                 |
| $L_s$              | Line Inductance                    | 10 $\mu$ H            |
| $R_s$              | Line resistance                    | 0.5 $\Omega$          |
| $R_{non}, L_{non}$ | Non-linear Load                    | 10 $\Omega$ , 16 mH   |
| $R_L, L_L$         | load Resistance, Inductance        | 20 $\Omega$ , 0.05 mH |
| $L_{se}$           | Switching ripple filter inductance | 5 mH                  |
| $Filter$           | Power factor capacitor Capacitance | 228 $\mu$ F           |
| $pf$               | Load power factor                  | 0.8 lag               |

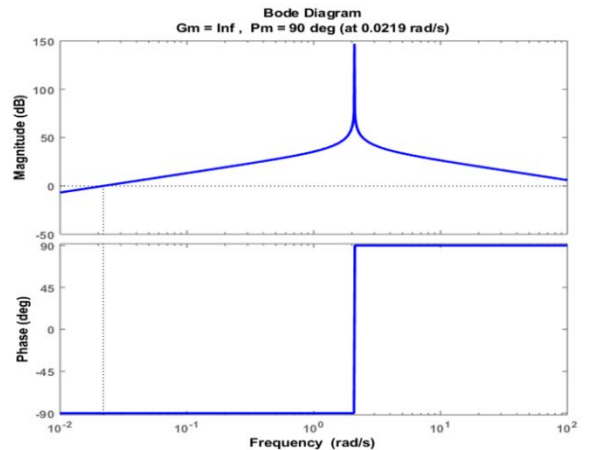


Figure 6. Frequency response of single-phase ShAPF.

A high nonlinearity is observed in source current in three phases (*A*, *B* and *C*). THD percentage of 16.7753 is observed in the source current waveform in phase *A*. According to the IEEE standards, it is not safe to operate the linear loads and sensitive loads supplying this non-linear current (Satish Kumar Gudey et.al 2014), (Satish Kumar Gudey et.al 2015). Hence, an appropriate filter should be tuned to inject the compensating current with exactly 180 degrees phase shift to nullify this harmonic current. Fig. 8 (b) shows the harmonic spectrum of the non-linear source current.

**6.1 Rectifier with R-Load**

Assume that linear and non-linear load (assume that there will be a three-phase bridge rectifier connected to a Resistive load) is connected at the PCC. The load voltages and load currents at the linear load are as shown in Fig. 9. The magnitudes of the load voltage and current are 100 V (rms), 15 A (rms). Figure 10 shows the current through the non-linear load, the compensated current, current drawn from the source.

It is observed that the source current THD is 0.75%, which is compensated by the ShAPF. Thus, the polluted THD content is reduced by using the ShAPF and is kept under the regulations imposed by the IEEE standards.

**6.2 Rectifier with RL-Load**

Now with the rectifier RL load, the THD of the source current is observed to be 22.44%. Now the ShAPF is connected to the circuit and simulated. The Three-phase voltage at load and phase currents through the linear load is shown in Fig. 12.

Figure 12 shows the waveforms for load voltage and current when the systems are fed with a rectifier with RL-load. The magnitudes of the load voltage are 100V (rms) and the magnitude of load current at the PCC is 10.25A (rms).

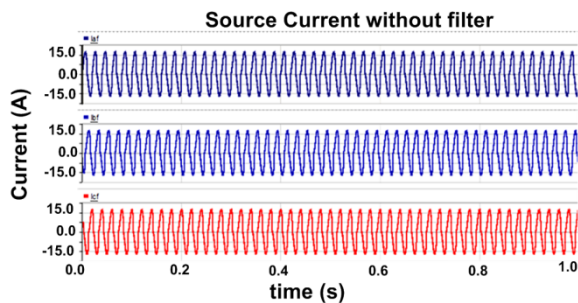


Figure 7. The waveform of the source current is in phases *A*, *B* and *C*.

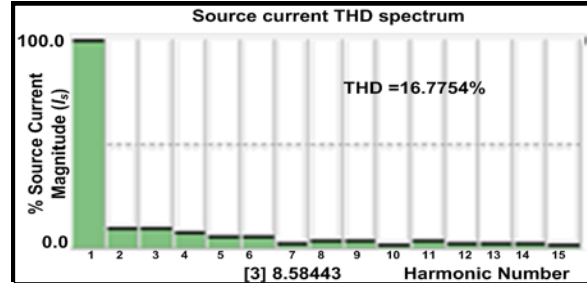
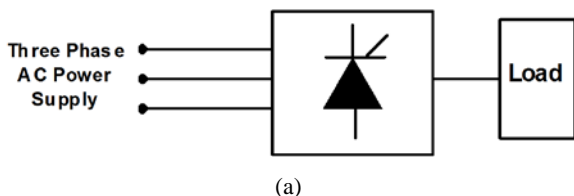


Figure 8. (a) Three-phase Thyristor bridge rectifier as Non-Linear Load, and (b) THD spectrum in the source current.

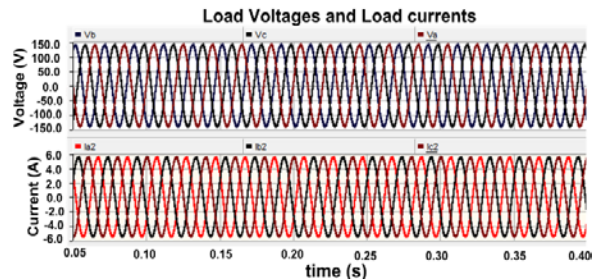


Figure 9. Three-phase waveforms of (a) voltage at load, and (b) linear load current.

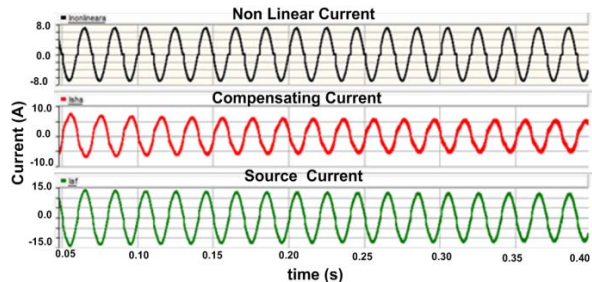


Figure 10. The waveform of current drawn by the non-linear load  $I_{nL}$ , shunt APF current  $I_{AF}$ , source current  $I_s$ .

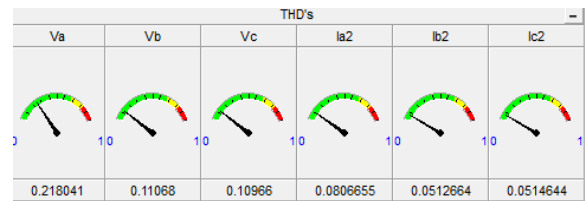


Figure 11. THD in load voltages and load currents.

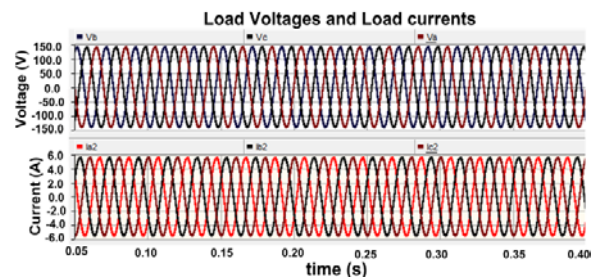
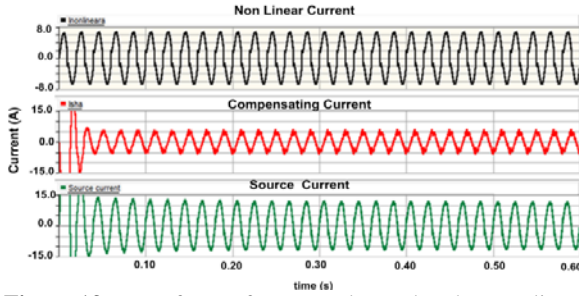
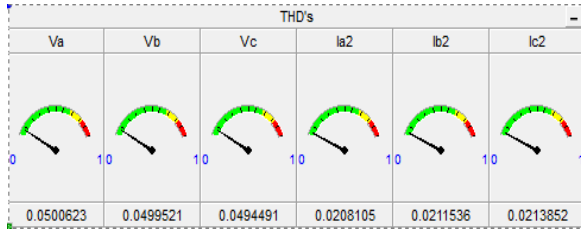


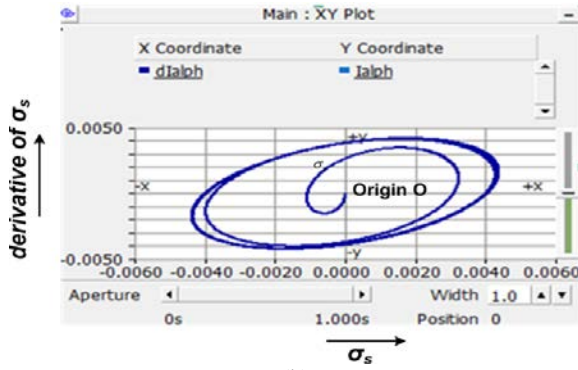
Figure 12. Three-phase Waveforms of voltage at load and phase currents drawn by the linear load.



**Figure 13.** Waveform of current drawn by the non-linear load  $I_{nL}$ , shunt APF current  $I_{AF}$ , source current  $I_s$ .



(a)



(b)

**Figure 14.** (a) THD in three-phase voltages and three-phase currents through the linear load, and (b) Phase plane projection of sliding surface  $\sigma_s$  and its derivative through simulation.

**Table 2.** Source Current THD with a non-linear load connected firing angle of  $36^\circ$ .

| S. No. | Resistance ( $\Omega$ ) | Inductance (mH) | % of THD in source current |
|--------|-------------------------|-----------------|----------------------------|
| 1      | 16                      | 16              | 1.21                       |
| 2      | 16                      | 20              | 0.88                       |
| 3      | 20                      | 16              | 1.06                       |
| 4      | 20                      | 24              | 0.75                       |
| 5      | 24                      | 24              | 0.75                       |

From Fig. 14(a) it is clear that the designed shunt APF is injecting the compensating current to maintain the THD in the load current within the permissible limits. SMC along with the ShAPF is said to work well in compensating the current harmonics. Figure 14 (b) shows the locus of the sliding surface  $\sigma_s$  with its derivative. The system reaches origin within a finite

period of 3 ms with high-frequency oscillations i.e. chattering is present in SMC (Vinay Kumar Naguboina et.al 2018). The chattering and hence, the settling time can be reduced by using an enhanced exponential sliding Mode controller (EERL-SMC) as discussed in section VII.

## 7. EER-LAW-BASED SLIDING MODE CONTROL FOR ShAPF

The chattering effect is the main drawback of the conventional SMC's. This had led the researchers to concentrate on higher-order SMC, which can avoid this chattering effect. In this paper the Enhanced Exponential Reaching Law is added to the existing conventional SMC to decrease the settling time, steady-state error, reducing response time (Quoc-Nam Trinh, et al. 2014): Hence, EERL based SMC can be used as an alternative instead of going for the higher-order SMC, which is presented in this proposed work. Here in this case the sliding surface  $s$  chosen is as shown in (10). Exponential reaching will have a high adaptive function when it is compared with the traditional controllers. The error signal obtained at the sliding surface will be given to the EERL as shown in Fig. 15. The equation of EERL-SMC is as shown in Equation (10).

$$\dot{s} = -\lambda s - \left( \frac{\xi}{D(s)} |s|^\gamma \cdot \text{sgn}(s) \right) \quad (10)$$

Here  $D(s) = \alpha + (1 - \alpha)e^{-\beta_x |s|} > 0$

The stability of the system will not depend on the value of  $D(s)$ . The values of  $\lambda$ ,  $\xi$  and  $\beta_x$  are always positive integers. Their values are in the range of 0 and 1. The time for reaching the system depends on  $|s|$ . As the value  $|s|$  decreases, the chattering effect can be minimized. The  $S_{\alpha\beta}$  obtained is passed through (10) and converted to  $S_{abc}$ , which is then compared with a repetitive waveform operating at 10 kHz to create the triggering pulses to the VSI circuit. The simulation results were obtained by adding the Exponential Reaching Law (Vinay Kumar Naguboina et.al 2018), (Mozayan et.al 2016), (Nayak V et.al 2020) to the presented SMC is given in sections 7.1 and 7.2.

### 7.1 Non-Linear load (R-Load)

In this simulation, only the non-linear load of 15A (max. value) is connected at the PCC. Then the resultant current drawn from the source is observed.

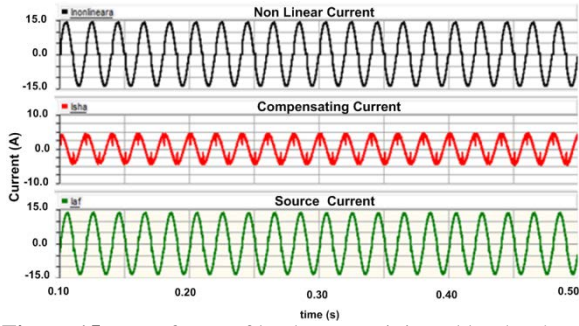


Figure 15. Waveforms of load, current injected by the shunt APF and Source current.

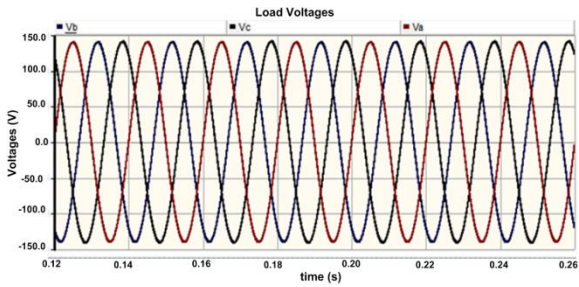


Figure 16. Three-phase voltages at the load.

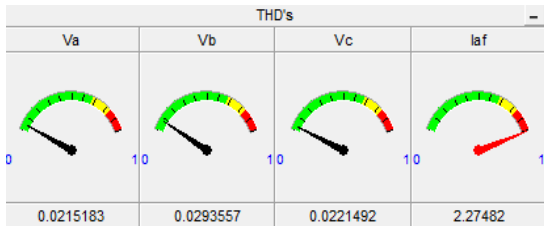


Figure 17. THD in Load Voltage and source current.

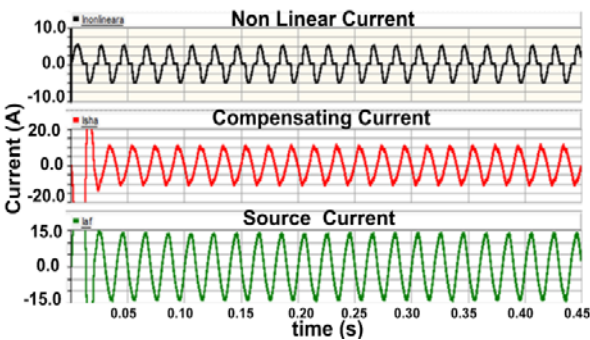


Figure 18. The waveform of the current is drawn by the non-linear load for a firing angle of 90 degrees, current injected by the shunt APF, source current.

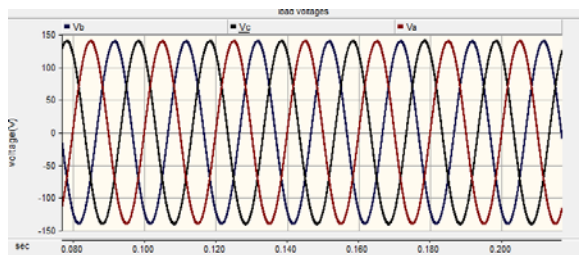


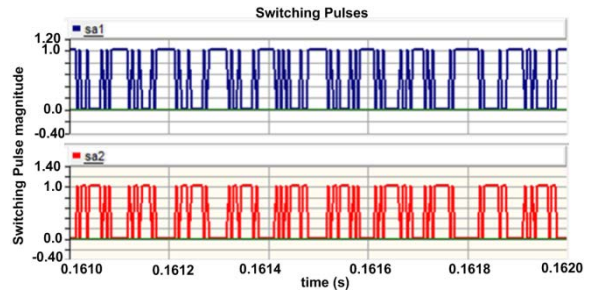
Figure 19. Waveforms of Load voltage.

From simulation results shown in Figs. 15,16, and 17, it is clear that the source current is free of harmonics. The harmonic content in the source is reduced to 2.27%, which is kept under regulation as per IEEE standard. Also, the THD in voltage at the PCC is within the allowable limits as per the standards.

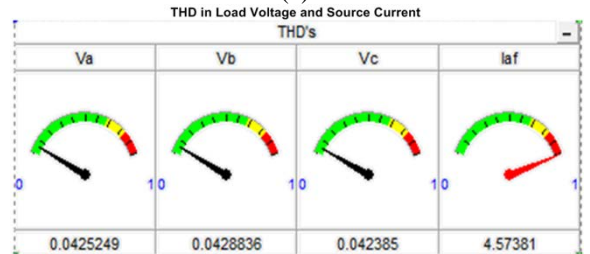
### 7.2 Non-Linear load (RL-Load)

The performance of the designed controller with EERL-SMC is analyzed by connecting the Non-Linear load with RL-load (Zobaa et.al 2014). In this simulation, a controlled rectifier is operated at a firing angle of 90 degrees. The resultant waveforms obtained is represented in Figure 18.

The designed filter is tested by changing the load parameters. The non-linear load (controlled rectifier fed RL load) is connected at the PCC. The controlled rectifier is operated at a firing angle of  $\alpha=36^\circ$ . The variation in the percentage of THD in the source current is observed and is listed in Table 4.



(a)



(b)

Figure 20. (a) Switching pulses generated by the controller, and (b) THD in load voltage and source current.

Table 3. Percentage of THD in Load phase voltages Va,Vb,Vc, Source Current.

| Type of Load | Va     | Vb     | Vc      | Is    |
|--------------|--------|--------|---------|-------|
| R-Load       | 0.0215 | 0.0293 | 0.02214 | 2.274 |
| RL-Load      | 0.0425 | 0.0428 | 0.0423  | 4.573 |

Table 4. Source Current THD with Non-linear load Connected to RL-Load Operated at  $\alpha=36^\circ$ .

| S.No. | Resistance ( $\Omega$ ) | Inductance (mH) | % of THD in source current |
|-------|-------------------------|-----------------|----------------------------|
| 1     | 16                      | 16              | 3.12                       |
| 2     | 16                      | 20              | 3.62                       |
| 3     | 20                      | 16              | 2.42                       |
| 4     | 20                      | 24              | 2.89                       |
| 5     | 24                      | 24              | 2.22                       |

Thus, by analyzing the simulation results it can be concluded that the designed ShAPF is having the capability to inject the compensating current whenever it is needed. Thus, it can be concluded that the designed ShAPF can act dynamically and mitigate the current distortions, which occur in the system. The convergence plot of the controller is drawn by considering the sliding surface on the X-axis and its derivative on the Y-axis. Then the resultant plot obtained is as shown in Fig. 21.

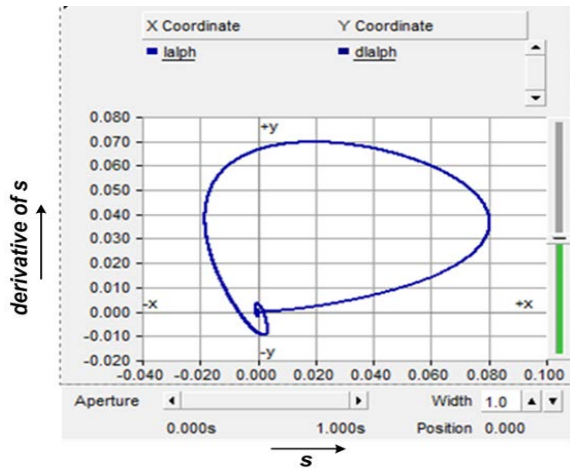


**Figure 21.** Phase plane projection of sliding surfaces and their derivative through simulation.

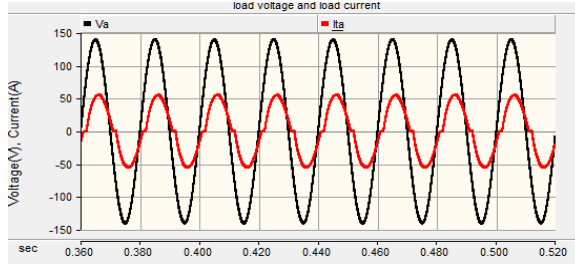


**Figure 22.** Load voltage and load current with only non-linear load at PCC.

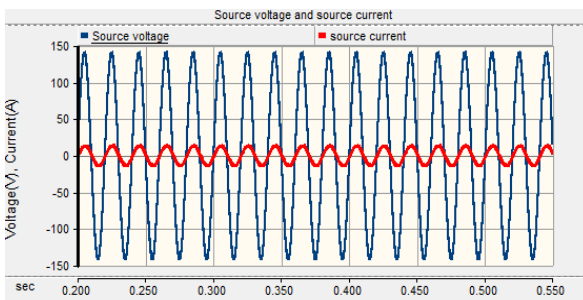


**Figure 23.** Source voltage and current.

**Table 5.** Comparison of SMC and EERL-SMC for a ShAPF.

| S.No. | Parameters               | SMC   | EERL-SMC |
|-------|--------------------------|-------|----------|
| 1     | % of THD in load current | 0.053 | 0.056    |
| 2     | % of THD in load voltage | 0.21  | 0.22     |
| 3     | settling time            | 3 ms  | 0.1 ms   |

The resultant is converging towards the origin, which indicates that the system is stable. The convergence time taken by the controller with EERL-SMC is quite less i.e. 0.1 ms when the phase plots of the controller with and without EERL are compared. Thus, it can be concluded that the controller with EERL shows less response time of 0.1 ms when compared with SMC, which converges in 3 ms. The chattering effect is also reduced as indicated in the waveforms obtained through simulation.

Figure 22 shows the load phase voltage of 100 V (rms) and load phase current of 3.97 A (rms) when a non-linear load is placed at PCC. The controller effectively improves the source current waveform to be sinusoidal as shown in Fig. 23. Table 5 shows the performance comparison of SMC and EERL-SMC. Both of them work effectively to maintain the THD within permissible limits. The EERL-SMC is better with less settling time during convergence.

## 8. CONCLUSION

In this article, a Shunt Active Power Filter in an EDS performance is simulated by connecting the non-linear load at the PCC. Both the conventional SMC and EERL-SMC are used to compensate for the effects of connected non-linear load at the PCC. It was identified that the proposed filter is functioning effectively to mitigate the polluted content in the source current. The current references are generated using the instantaneous  $P-Q$  theory. The proposed controller for ShAPF is tested in three-phase systems by connecting  $R$  and  $RL$  elements on the DC side to the Non-linear load. For the proposed system, the polluted content in voltage and current is reduced and is regulated by the controller. The THD obtained using both the controllers are kept under the limitations imposed by the IEEE standards. It highlights the need for a reliable power supply for critical loads and with an increase in the number of non-linear loads. The stability of the system is analyzed using frequency response characteristics. It is found that the system is stable. The finite-time convergence is indicated through a phase plot, which realizes a faster settling time of 0.1 ms using EERL-SMC compared to 3 ms in a conventional SMC. The EERL-SMC is an alternative to the higher-order SMC for chattering reduction and finite-time convergence. The main applications of ShAPF are in PV systems, smart grid networks, distributed generation and machine control.

## CONFLICT OF INTEREST

The authors declare no conflict of interest.

## FUNDING

No funding was received for this study.

## REFERENCES

- Alireza Javadi, Lyne Woodward, and Kamal Al-Haddad (2017).: Real-time Implementation of a Three-phase THSeAF Based on VSC and P+R controller to Improve Power Quality of Weak Distribution Systems”, IEEE Trans. On Power Electronics., 33(3): pp. 2073-2082.
- Alireza Javadi, Handy Fortin Blanchette, and Kamal Al-Haddad (2012): A Novel Transformerless Hybrid series Active Filter, IEEE Trans. On Power Electronics,99, 5312-5317.
- Alireza Javadi, and Kamal Al-Haddad, Kouro, S (2015), A Single-Phase Active Device For Power Quality Improvement of Electrified Transportation, IEEE Transactions on Industrial Electronics, 62, 3033-3041.
- Ghosh, A, Jindal, A. K. and Joshi, A (2004), “Design of a capacitor supported dynamic voltage restorer (DVR) for unbalanced and distorted loads,” Power Delivery, IEEE Transactions on, 19, pp. 405-413.
- Gupta, R, Ghosh, A., and Joshi, A (2011), “Performance comparison of VSC based shunt and series compensators for load voltage control of distribution systems”, in IEEE transactions on power delivery, 26(1).
- Thentral, T. M. T. *et al.*, (2021) “Development of Control Techniques Using Modified Fuzzy Based SAPF for Power Quality Enhancement,” in IEEE Access, 9, 68396-68413.
- Javadi, A., Hamadi, A, Ndtoungou, A and Al-Haddad, K (2017): Power Quality Enhancement of Smart Households Using a Multilevel-THSeAF With a PR Controller, IEEE Transactions on Smart Grid., 8, 465-474.
- Javadi, A, Lyne Woodward and Al-Haddad, K, (2016) “Experimental Investigation on a Hybrid Series Active Power Compensator to Improve Power Quality of Typical Households”, IEEE Transactions on Industrial Electronics, vol. pp.
- Mozayan, S. M., Saad, M., Vahedi, H., Fortin-Blanchette, H. and Soltani, M., (2016) “Sliding Mode Control of PMSG Wind Turbine Based on Enhanced Exponential Reaching Law,” in IEEE Transactions on Industrial Electronics, vol. 63, no. 10, pp. 6148-6159.
- Ma, H., Li, Y., Xiong, Z. (2019) “Discrete-Time Sliding-Mode Control With Enhanced Power Reaching Law,” in IEEE Transactions on Industrial Electronics, 66(6), 4629-4638.
- Ma, H., Wu, J., Xiong, Z. (2017)“A Novel Exponential Reaching Law of Discrete-Time SlidingMode Control”, IEEE Transactions on Industrial Electronics, 64(5), 3840-3850.
- Nayak V and Satish Kumar Gudey (2020) “An Enhanced Exponential Reaching Law-Based SMC for a UPS system in Industrial Applications,” in Serbian Journal of Electrical Engineering, Vol. 17, No. 3, October 2020, 313-336.
- Ouchen, S., Benbouzid, M. Blaabjerg, F. Betka, A. and Steinhart, H. (2021) “Direct Power Control of Shunt Active Power Filter Using Space Vector Modulation Based on Supertwisting Sliding Mode Control,” *in* IEEE Journal of Emerging and Selected Topics in Power Electronics, 9(3), 3243-3253
- Quoc-Nam Trinh, Hong-Hee Lee (2014): Improvement of unified power quality conditioner performance with enhanced resonant control strategy, IET Gener Transm. Distrib., 8(12), 2114-2123.
- Rashid M. H. (2011) Power electronic converters handbook 3<sup>rd</sup> edition, Elsevier, chapter-41, pp.1215-1216.
- Satish Kumar Gudey and Rajesh Gupta (2014), “Sliding mode control in voltage Source inverter-based high-order circuits, International Journal of Electronics, vol. 102, no. 4, pp. 668-689.
- Satish Kumar Gudey and Rajesh Gupta (2014), “Sliding mode control of DVR For mitigation of Source Side Voltage Disturbances”, International Conference on standards for smart grid Ecosystem, 6-7 march Bangalore.
- Satish Kumar Gudey and Rajesh Gupta (2015) “Reduced state feedback sliding-mode current control for voltage source inverter-based higher-order circuit”, IET Power Electron., 8 (8), 1367-1376.
- Sharma, S, Verma, V and Behera, R. K. (2020) “Real-Time Implementation of Shunt Active Power Filter With Reduced Sensors,” in IEEE Transactions on Industry Applications, 56(2), 1850-1861.
- Vinay Kumar Naguboina, Satish Kumar Gudey (2018), “A Compensation Strategy Using THSeAF in a Distribution System based on SMC for Source side and Load side Control” – IEEE International Conference on Computing, Power and Communication technologies – 27<sup>th</sup> & 28<sup>th</sup> September, Galgotias University, vol.pp.433-438.
- Vinay Kumar Naguboina, Satish Kumar Gudey, (2018), “Enhanced Exponential Reaching Law SMC for Analyzing PQ Issues in a distribution System using ThSeAF” – Indian Council International Conference (INDICON) – 15<sup>th</sup>to 18<sup>th</sup> December, IIT Madras, vol.pp.1-6.
- Zobaa, A. F. (2014), “Optimal multiobjective design of hybrid active power filters considering a distorted environment”, IEEE Trans. Ind. Electron., 61, pp. 107-114.